

Nitric oxide-induced genotoxicity, mitochondrial damage, and apoptosis in human lymphoblastoid cells expressing wild-type and mutant p53

Chun-Qi Li, Laura J. Trudel, and Gerald N. Wogan*

Biological Engineering Division and Department of Chemistry, Massachusetts Institute of Technology, Cambridge, MA 02139

Contributed by Gerald N. Wogan, June 14, 2002

Nitric oxide (NO[•]) is mutagenic and, under appropriate conditions of exposure, also induces apoptosis in many *in vitro* and *in vivo* experimental models. Biochemical and cellular mechanisms through which NO[•] induces apoptosis are incompletely understood, but involve p53/mitochondria-dependent signaling pathways. In this study, we exposed human lymphoblastoid cells harboring either wild-type (TK6 cells) or mutant p53 (WTK-1 cells) to NO[•], delivered by diffusion through Silastic tubing. Cells were exposed for 2 h at constant rates of 100–533 nM/s, similar to levels estimated to occur *in vivo* in inflamed tissues. DNA double-strand breaks and fragmentation detected 8–48 h after NO[•] treatment were more extensive in TK6 cells than in WTK-1 cells, whereas NO[•]-induced mutant fractions in both *HPRT* and *TK1* genes were significantly lower in TK6 cells than in WTK-1 cells ($P < 0.01$ – 0.05). Treatment of TK6 cells with NO[•] caused extensive apoptosis, but this response was delayed and greatly reduced in magnitude in WTK-1 cells. Mitochondrial membrane depolarization and cytochrome *c* release were induced in both cell types. However, elevation of apoptotic protease-activating factor-1 (Apaf-1) protein and reduction of X-chromosome-linked inhibitor of apoptosis (XIAP) protein were observed only in TK6 cells. These results indicate that p53 status is an important modulator of NO[•]-induced mutagenesis and apoptosis, and suggest that levels of the Apaf-1 and XIAP proteins, but not mitochondrial depolarization and cytochrome *c* release, are regulated by p53 in these human lymphoblastoid cells. Thus, Apaf-1 and XIAP may play important roles in the regulation of p53-mediated apoptotic responses.

Extensive evidence indicates that nitric oxide (NO[•]) is cytotoxic and mutagenic, and that its effects on apoptosis are variable depending on NO[•] doses and cell types. It promotes apoptosis in many cell types, whereas in others, including hepatocytes, it inhibits the induction of apoptosis by drugs or growth factor withdrawal (1, 2). Apoptotic signaling pathways initiated by NO[•] have not been fully elucidated, but are known to involve p53 accumulation (3) and changes in mitochondrial function (4). Two major signaling pathways leading to apoptosis have been identified in both *in vitro* and *in vivo* experimental models. One is p53/mitochondria-dependent, involving release of cytochrome *c* and leading to caspase activation through the apoptotic protease-activating factor-1 (Apaf-1) (5, 6). The other is Fas/caspase-8-dependent, involving interaction of the death receptor proteins with the receptor-associated death proteases and subsequent activation of downstream effector caspases (7). In addition, inhibitors of apoptosis (IAP) genes have been identified in baculoviruses and in mammalian cells and have been shown to suppress apoptosis induced by a variety of stimuli by selectively inhibiting distinct caspases (8).

Wild-type p53 gene product is known as a critical cellular gatekeeper for growth and division by regulating transcription of genes involved in growth arrest, DNA repair, apoptosis, and gene amplification (9, 10). For example, ionizing radiation and DNA-damaging agents have been shown to induce earlier apoptosis in human lymphoblastoid TK6 cells harboring wild-type p53 than in WTK-1 cells carrying mutant p53 (11–15). However, WTK-1

cells were about 20 times more sensitive to mutagenesis induced by 1.5-Gy x-rays and also showed a 10-fold higher spontaneous mutation rate at the autosomal heterozygous *TK1* locus (16). In addition, mismatch-repair capacity was a strong determinant of the susceptibility of these cells to alkylation-induced apoptosis (17). Recently, Apaf-1 and caspase-9 were found to be essential downstream components of p53 in Myc-induced apoptosis (18), and Apaf-1 protein deficiency conferred resistance to cytochrome *c*-dependent apoptosis in human leukemia cells (19).

Both dose and delivery method can significantly affect responses to NO[•] in experimental systems, resulting in conflicting findings regarding its effects on such parameters as cytotoxicity and apoptosis. In some studies, cells have been exposed by means of donor drugs to total NO[•] doses orders of magnitude higher, and at different rates, than those estimated to occur *in vivo* (20). In addition, because their reactivity may be quite distinct from that of NO[•], the possibility cannot be excluded that some cellular responses may, at least in part, be attributable to the drugs themselves or to their decomposition products (21, 22).

We undertook this study to investigate genotoxicity, mitochondrial damage, and apoptosis induced by NO[•] in human lymphoblastoid cells expressing either wild-type (TK6 cells) or mutant p53 (WTK-1 cells). WTK-1 cells contain a T-to-C transition in exon 7 of the *p53* gene, resulting in a substitution of *Ile* for *Met* at codon 237 (11–15). NO[•] was delivered into stirred cell suspensions by diffusion through Silastic tubing at a constant rate and at levels similar to those estimated to occur *in vivo* in inflamed tissues (23). TK6 and WTK-1 cells were selected principally because they have been used extensively to characterize spectra of mutations induced at two loci by many types of mutagens, and because they share a common genetic origin. We found that DNA double-strand breaks and fragmentation after NO[•] treatment were more extensive in TK6 cells than in WTK-1 cells. Induced and spontaneous mutant fractions (MF) in hypoxanthine-guanine phosphoribosyltransferase (*HPRT*) and thymidine kinase (*TK1*) genes were lower in TK6 than in WTK-1 cells. NO[•] caused early and extensive apoptosis in TK6 cells, whereas this response was delayed and diminished in WTK-1 cells. In contrast, extensive mitochondrial membrane depolarization and cytochrome *c* release resulted from NO[•] treatment in both cell types. Increased expression of the Apaf-1 protein and decreased expression of the X-chromosome-linked IAP (XIAP) protein followed NO[•] treatment in TK6 cells but not in WTK-1 cells. Collectively, these findings emphasize the importance of p53 status as a determinant of mutagenic and apoptotic responses to DNA damage induced by NO[•] in these two human

Abbreviations: Apaf-1, apoptotic protease-activating factor-1; *HPRT*, hypoxanthine-guanine phosphoribosyltransferase gene; IAP, inhibitor of apoptosis; JC-1, 5,5',6,6'-tetrachloro-1,1',3,3'-tetraethylbenzimidazolylcarbocyanine iodide; MF, mutant fraction; MMP, mitochondrial membrane potential; NO[•], nitric oxide; *TK1*, thymidine kinase gene; TK6 cells, human lymphoblastoid TK6 cells; WTK-1 cells, mutant p53 human lymphoblastoid cells; XIAP, X-chromosome-linked inhibitor of apoptosis protein; 4-NQO, 4-nitroquinoline 1-oxide.

*To whom reprint requests should be addressed. E-mail: wogan@mit.edu.

lymphoblastoid cell lines and suggest that Apaf-1 and XIAP may also play important roles in p53-mediated apoptosis.

Materials and Methods

Materials. Pure NO[•] gas was purchased from Matheson. TK6 cells were kindly provided by W. G. Thilly (Massachusetts Institute of Technology), and WTK-1 cells by H. Liber (Massachusetts General Hospital). All cell culture reagents were purchased from BioWhittaker. ApoAlert annexin V-FITC kit was from CLONTECH. Quick apoptotic DNA ladder detection kit (BioVision) was purchased from Alexis Biochemicals, San Diego. Comet assay kit was obtained from Trevigen (Gaithersburg, MD). 5,5',6,6'-Tetrachloro-1,1',3,3'-tetraethylbenzimidazolyl-carbocyanine iodide (JC-1) was supplied by Molecular Probes. Hoechst 33258, propidium iodide, etoposide, 6-thioguanine, trifluorodeoxythymidine, rat heart cytochrome *c*, and trypan blue were obtained from Sigma. Mixture of protease inhibitors was purchased from Roche Diagnostics. Bio-Rad protein assay, Laemmli sample buffer, SDS-15% polyacrylamide gel, polyvinylidene difluoride membrane, goat and rabbit anti-mouse IgG conjugated to horseradish peroxidase were obtained from Bio-Rad. Monoclonal anti-cytochrome *c* antibody 7H8.2C12, monoclonal anti-human Apaf-1 antibody clone 24, and 4 μ M staurosporine-treated Jurkat cell lysates were purchased from PharMingen. Polyclonal anti-human XIAP antibody was provided by Cell Signaling Technology (Beverly, MA). Monoclonal anti-actin antibody (clone 14) was purchased from Chemical Credential (Aurora, OH). SuperSignal chemiluminescence was obtained from Pierce. Hyperfilm ECL was obtained from Amersham Pharmacia. Silastic tubing (0.025 inches i.d., 0.047 inches o.d.) was obtained from Dow Corning.

Cell Culture. TK6 and WTK-1 cells were maintained in exponentially growing suspension culture at 37°C in a humidified, 5% CO₂ atmosphere in RPMI medium 1640 supplemented with 10% heat-inactivated calf bovine serum, 100 units/ml penicillin, 100 μ g/ml streptomycin, and 2 mM L-glutamine. Stock cells were subcultured and maintained at a density not greater than 1×10^6 cells per ml in 150-mm dishes during experiments.

NO[•] Treatment. Cells at a density of 4×10^5 cells per ml in 100 ml of custom RPMI medium 1640 without calcium nitrate (GIBCO) and calf serum were exposed to NO[•] through Silastic tubing in the membrane delivery system as described (23). NO[•] diffuses through this permeable tubing at a constant rate, and was delivered into the medium of well stirred cell suspensions at dose rates controlled by varying the tubing length from 5 to 30 cm. Cells exposed to argon gas through 30-cm tubing served as negative controls. All exposures were 2 h in length. Total amounts of NO[•] delivered under these conditions, expressed as nitrite plus nitrate concentrations, were quantified by automated analysis by using the Griess reagent [*N*-(1-naphthyl)-ethylenediamine and sulfanilic acid] as described (24). At the end of treatment, cells were collected by centrifugation, washed once, resuspended in fresh culture medium, and incubated at 37°C.

Analysis of Cell Survival. We first compared NO[•]-induced cell lethality determined by trypan blue exclusion with that determined by plating efficiency (25) and found that both methods produced similar survival values 8 and 24 h after treatment. Therefore, in this study survival was determined by staining cells with 0.4% trypan blue solution followed by enumeration of those excluding the stain under a phase-contrast microscope.

Determination of Mutant Fraction. NO[•]-treated cells were grown for 6–10 days to allow phenotypic expression and then plated in selective medium for MF determination. A total of 24×10^6 cells from each treatment group were transferred to ten 96-well plates

at densities of 40,000 cells per well in medium containing 6-thioguanine (2 μ g/ml) to select *HPRT* mutants or trifluorothymidine (2 μ g/ml) to select *TK1* mutants. For plating efficiency analysis, 120 cells in 12 ml of nonselective medium from each group were plated in duplicate in 96-well plates at a density of one cell per 100 μ l per well. After 2 weeks of incubation, colonies were counted and MF was calculated according to the described method (25). In parallel experiments, to estimate spontaneous mutation rate and to determine response of the *HPRT* and *TK1* genes to treatment with a well characterized mutagen, similar MF analyses were done on untreated cells and cells treated with 4-nitroquinoline 1-oxide (4-NQO) (140 ng/ml for 1.5 h) as described above.

Neutral Single-Cell Gel Electrophoresis (Comet Assay). Neutral comet assays were performed by using the Trevigen CometAssay kit to assess NO[•]-induced DNA double-strand breaks. Cells at 1×10^5 /ml were combined with molten LMAgarose (at 42°C) at a ratio of 1 to 10, and 50 μ l were immediately pipetted onto a CometSlide. The slides were kept at 4°C for 10 min, lysed for 1 h in prechilled lysis buffer [2.5 M sodium chloride/100 mM EDTA (pH 10)/10 mM Tris base/1% sodium lauryl sarcosinate/0.01% Triton X-100], then electrophoresed at 30 V for 20 min. After staining with SYBY Green, cells were photographed under a fluorescence microscope and analyzed with the Komet 4.2 Single Cell Gel Electrophoresis Analysis (Kinetic Imaging Limited, Liverpool, U.K.). Olive tail moment, defined as the product of percentage DNA in the tail and displacement between the position of the mean centers of mass in the heads and tails (26), was determined for at least 40 cells per sample. Cells treated with argon gas were used as negative controls, and cells treated with 1–100 μ M H₂O₂ in RPMI medium 1640 for 20 min at 4°C as positive controls.

DNA Fragmentation Analysis. DNA fragmentation in cells treated with NO[•] was detected by agarose gel electrophoresis by using a DNA ladder detection kit according to the recommended procedure. In brief, 1×10^6 cells were lysed with TE lysis buffer and DNA was extracted. Two micrograms of DNA were loaded on 1% agarose gel, run at 50 V for 2 h in $1 \times$ TBE buffer (100 mM Tris/90 mM boric acid/1 mM EDTA, pH 8.4) with 0.5 μ g/ml ethidium bromide, and photographed.

Apoptosis Analysis. Morphological changes in apoptotic cell nuclei were detected by microscopic examination of cells stained with Hoechst 33258. Quantitative estimation of apoptosis was accomplished by flow cytometry after annexin V-FITC staining, as described in the kit instructions. One milliliter of cell suspension was washed once with annexin-binding buffer and resuspended in 200 μ l of binding buffer. Cells were stained for 15 min at room temperature in the dark with annexin V-FITC to a final concentration of 0.5 μ g/ml, and propidium iodide to a final concentration of 2.5 μ g/ml. The volume was adjusted to 600 μ l by using ice-cold binding buffer and analyzed by a Becton Dickinson FACScan (excitation light, 488 nm) equipped with CELLQUEST software. Annexin V-FITC fluorescence was recorded in FL-1 and propidium iodide in FL-2. Early apoptotic cells were labeled with only annexin V, necrotic cells were stained with propidium iodide or with both annexin V and propidium iodide, and living cells were negative for both staining. Cells treated with argon gas served as negative controls, and those treated with 2.5 μ M etoposide in culture medium for 6 h as served as positive controls.

Mitochondrial Membrane Potential (MMP) Analysis. Aliquots of cell suspensions were incubated with 10 μ M JC-1, a specific MMP-dependent fluorescence dye (27), for 30 min at 37°C and washed three times in PBS. Mitochondrial depolarization was qualita-

tively estimated by fluorescence microscopy with a long-pass filter (28) or quantitatively measured by flow cytometry as described (29). JC-1 exhibits dual fluorescence emission depending on MMP state. JC-1 forms aggregates in cells with a high FL-2 fluorescence (585 nm) indicating a normal MMP. MMP loss results in a reduction in FL-2 fluorescence with a concurrent gain in FL-1 fluorescence (530 nm) as the dye shifts from aggregates to monomeric state. Therefore, retention of the dye in the cells can be monitored through the increase in FL-1 fluorescence. The data were converted to density plots by using CELLQUEST software for presentation. Cells treated with argon gas or with 2.5 μ M etoposide served as negative and positive controls, respectively.

Immunoblotting Analysis of Cytochrome *c*, Apaf-1, and XIAP. At the indicated times after NO \bullet treatment, cells were harvested, lysed in buffer A [250 mM sucrose/20 mM Hepes-KOH (pH 7.4)/10 mM KCl/1.5 mM Na-EGTA/1.5 mM Na-EDTA/1 mM MgCl $_2$ /1 mM DTT and mixture of protease inhibitors], and ground in a glass Dounce homogenizer with a tight pestle (B-type). Homogenates were centrifuged at 800 \times *g* for 10 min at 4°C. Supernatants were further centrifuged at 26,000 \times *g* for 20 min at 4°C (30). Protein concentration of the resulting supernatants (cytosolic fraction) was measured with the Bio-Rad protein assay for cytochrome *c* and Apaf-1 measurement. For XIAP analysis, whole-cell lysates were used. Proteins (25–50 μ g) were denatured, separated by SDS/15% PAGE, and electrotransferred to a polyvinylidene difluoride membrane. The blots were probed with monoclonal anti-cytochrome *c* antibody 7H8.2C12 (1:2,000 dilution), monoclonal anti-human Apaf-1 antibody clone 24 (1:250 dilution), or polyclonal anti-human XIAP antibody (1:1,000 dilution) for 2 h at room temperature or overnight at 4°C, followed by a secondary goat or rabbit anti-mouse IgG conjugated to horseradish peroxidase, and determination of supersignal ultrachemiluminescence. To control for similar protein loading, the membranes were stripped and reprobed with antiactin antibody (1:3,000 dilution).

Statistical Analysis. All experiments were repeated at least twice after experimental conditions were optimized. Statistical analysis was performed by using a two-tailed Student's *t* test, and *P* < 0.05 was considered to be statistically significant.

Results

Cytostasis. When cells were exposed to NO \bullet for 2 h, the NO \bullet exposure rates and cumulative doses (nitrite plus nitrate in the medium) at tubing lengths of 30, 15, and 5 cm were 533 nM/s (390 μ mol), 300 nM/s (210 μ mol), and 100 nM/s (70 μ mol), respectively; no nitrite or nitrate was detectable in the medium of cells treated with argon gas. As shown in Fig. 1, control TK6 and WTK-1 cells continued to grow exponentially after exposure to argon gas, with doubling times about 24 h. TK6 cells treated with NO \bullet at 100 nM/s showed a slightly reduced growth rate. NO \bullet had similar toxicity to TK6 and WTK-1 cells, in that cells treated with NO \bullet at 300 nM/s for 2 h grew very slowly, with a doubling time of about 60 h, and NO \bullet treatment at a higher rate (533 nM/s) induced cytostasis in both cell types.

Mutagenesis. Mutagenesis of the *HPRT* and *TK1* genes was determined in cells exposed to NO \bullet at 533 nM/s for 2 h. As shown in Fig. 2, in TK6 cells, MF increased 2-fold in the *HPRT* gene and 4.2-fold in the *TK1* gene compared with argon-treated controls (5.3×10^{-6} vs. 2.7×10^{-6} and 10.5×10^{-6} vs. 2.5×10^{-6} , respectively). WTK-1 cells treated under the same conditions showed increases in MF of 2.6-fold in the *HPRT* and 6.6-fold in *TK1*, respectively, when compared with controls (11.5×10^{-6} vs. 4.39×10^{-6} and 64.7×10^{-6} vs. 9.81×10^{-6}). By comparison, in 4-NQO-treated positive controls, induced MF

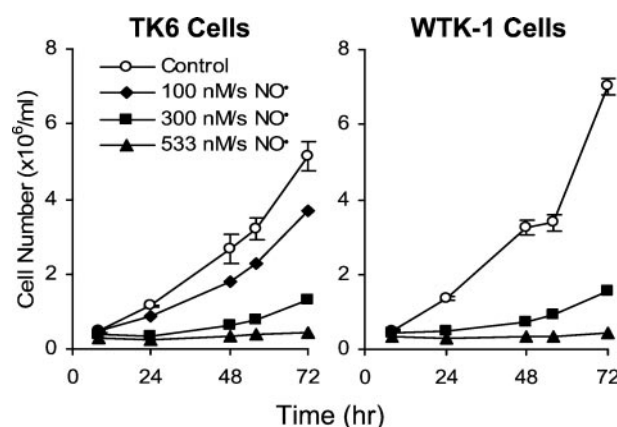


Fig. 1. Survival of TK6 and WTK-1 cells after NO \bullet treatment, as determined by trypan blue exclusion. Cells were exposed to varying rates of NO \bullet for 2 h. Cell survival after exposure to 100 nM/s NO \bullet was determined only in TK6 cells. Data represent the mean of two duplicate experiments. Standard deviations were less than 15% (not shown).

in the *HPRT* and *TK1* genes were 20.2×10^{-6} and 23.4×10^{-6} in TK6 cells and 25×10^{-6} and 72.3×10^{-6} in WTK-1 cells, respectively. Spontaneous as well as NO \bullet - and 4-NQO-induced MF were significantly higher in WTK-1 cells than in TK6 cells (*P* < 0.05–0.01), except in *HPRT* mutants induced by 4-NQO (*P* > 0.05). In addition, in WTK-1 cells, larger increases in MF in *TK1* than in *HPRT* were found both in spontaneous mutants and in those induced by NO \bullet or 4-NQO (*P* < 0.05–0.01).

DNA Double-Strand Breaks and Fragmentation. Induction of DNA double-strand breaks by NO \bullet was evaluated by neutral comet assay, with the results shown in Fig. 3. DNA tail moments were significantly increased in both TK6 and WTK-1 cells 8 h after treatment, compared with argon gas-treated controls. Frequency and severity of DNA damage were strongly increased by 24 and 48 h after NO \bullet treatment (data not shown). Olive tail moments were significantly higher in TK6 cells than in WTK-1 cells treated with NO \bullet at 533 nM/s for 2 h (8.6 ± 3.79 vs. 3.73 ± 2.19 , *P* < 0.05) or positive control cells treated with 100 μ M H $_2$ O $_2$ (18.8 ± 4.8 vs. 10.7 ± 3.1 , *P* < 0.01), but no significant differences in response were found in cells treated with 300 nM/s for 2 h or with 1 or 10 μ M H $_2$ O $_2$.

These results were further supported by gel electrophoretic analysis of DNA, which showed that DNA fragmentation was more extensive in TK6 cells than in WTK-1 cells. After treatment

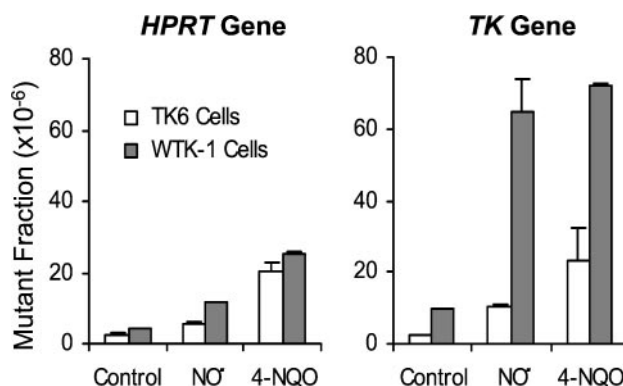


Fig. 2. Mutant fractions in the *HPRT* and *TK1* genes of TK6 and WTK-1 cells treated with NO \bullet at 533 nM/s for 2 h. Cells treated with argon gas or 4-NQO (140 ng/ml for 1.5 h) served as negative and positive controls, respectively. Results shown are mean \pm SD of duplicate experiments.

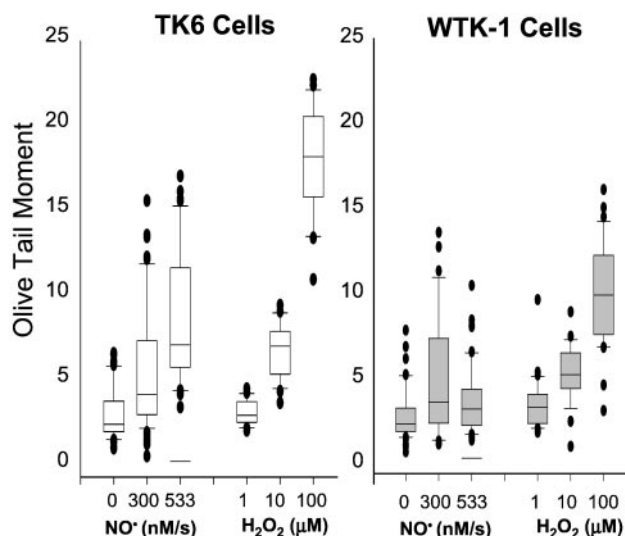


Fig. 3. Box-and-whisker plots of Olive tail moments from neutral comet assays of TK6 and WTK-1 cells 8 h after treatment with varying rates of NO[•] for 2 h. At least 40 cells were analyzed in each sample. Cells treated with argon gas or with H₂O₂ were used as negative and positive controls, respectively. Olive tail moments were significantly higher in TK6 cells than in WTK-1 cells treated with NO[•] at 533 nM/s ($P < 0.05$) or treated with 100 μ M H₂O₂ ($P < 0.01$), but differences between TK6 and WTK-1 cells treated with NO[•] at 300 nM/s or 1 and 10 μ M H₂O₂ were not significant ($P > 0.05$).

of cells with 300 nM/s, DNA fragmentation was evident in TK6 cells at 24 h but not in WTK-1 cells even at the longest time interval of 72 h after treatment. After exposure to 533 nM/s, DNA fragmentation was detected in WTK-1 cells at 72 h (Fig. 4), at which time no genomic DNA could be recovered from TK6 cells, probably because total DNA fragmentation.

Apoptosis. In preliminary experiments, we observed nuclear condensation and fragmentation in NO[•]-treated cells by fluorescence microscopy after Hoechst 33258 staining (data not shown). Subsequently, apoptosis was dynamically quantified by using flow cytometry after annexin-V staining, with the results shown in Fig. 5A. NO[•] induced significantly higher apoptosis in TK6 cells than in WTK-1 cells. Exposure of TK6 cells to 100 nM/s NO[•] induced a 2.0- to 2.5-fold elevation in the number of apoptotic cells compared with controls (data not shown), whereas exposure of WTK-1 cells to 300 nM/s induced only slightly increased apoptosis. TK6 cells underwent rapid onset of apoptosis that reached maximum frequency 32–56 h after treatment, depending on the dose of NO[•]. Maximum apoptotic frequency was 59% in TK6 cells treated with 533 nM/s, a 16-fold increase compared with controls. In WTK-1 cells, apoptotic

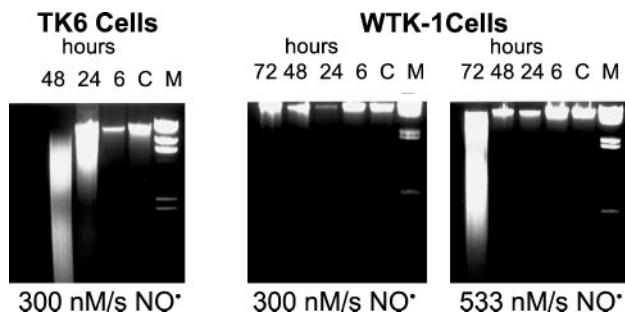


Fig. 4. DNA fragmentation in TK6 and WTK-1 cells treated with varying rates of NO[•] for 2 h, detected by agarose gel electrophoresis.

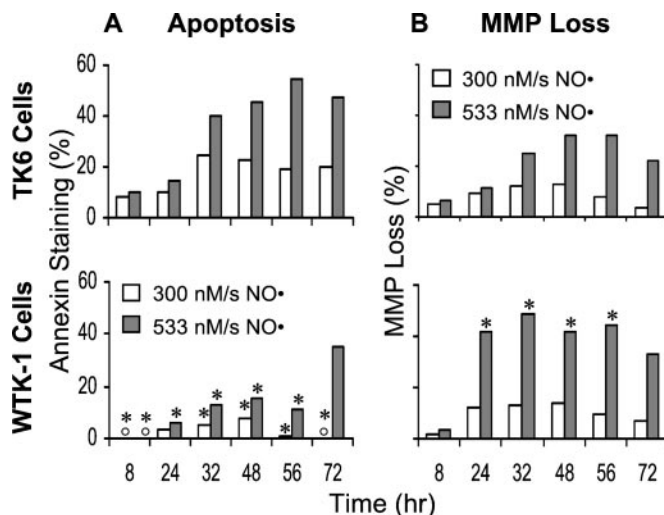


Fig. 5. Normalized apoptosis (A) and MMP loss (B) in TK6 and WTK-1 cells treated with varying rates of NO[•] for 2 h. Cells treated with argon gas were used as negative controls. Data represent the mean of two experiments, each done in duplicate. Standard deviations were 6–16% (not shown). *, $P < 0.04$ – 0.02 , compared with TK6 cells.

response was significantly reduced and delayed, peaking at 72 h after exposure to 533 nM/s, with a maximum frequency of 41% apoptosis, 9.6-fold higher than that in argon-treated cells.

Mitochondrial Membrane Depolarization. Qualitative evidence of mitochondrial depolarization (MMP loss) induced by exposure to NO[•] was observed by fluorescence microscopy in both TK6 and WTK-1 cells stained with JC-1. Aggregates of JC-1 in normal cells appeared red, whereas monomers in damaged cells with MMP loss appeared green (data not shown). Quantitative evaluation by flow cytometry revealed that NO[•] induced MMP loss in both cell types in a dose-dependent fashion, but to a significantly greater magnitude in WTK-1 cells 24–56 h after treatment (Fig. 5B). After exposing cells to NO[•] at 533 nM/s, MMP loss was observed as early as 8 h in both cell types and became more evident at 48 h in TK6 cells with a maximum MMP loss of 34%, or at 32 h in WTK-1 cells with a maximum MMP loss of 54%.

Cytochrome c Release, Apaf-1, and XIAP Expression. Changes in levels of cytochrome c as well as Apaf-1 and XIAP gene products after exposure of cells to NO[•] at a rate of 533 nM/s were determined by immunoblot analysis, with results summarized in Figs. 6, 7, and 8. Cytochrome c was released from mitochondria into the cytosol in both types of cells after NO[•] exposure.

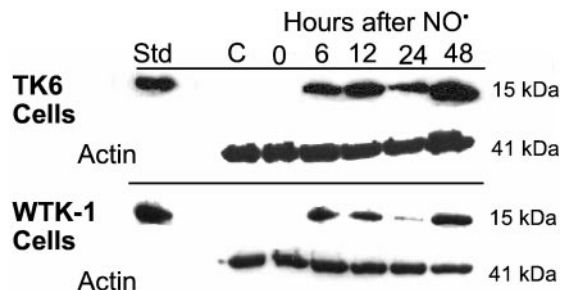


Fig. 6. Release of mitochondrial cytochrome c into cytosol in TK6 and WTK-1 cells treated with NO[•] at 533 nM/s for 2 h, detected by Western blots. Rat heart cytochrome c (25 ng) served as a positive control.

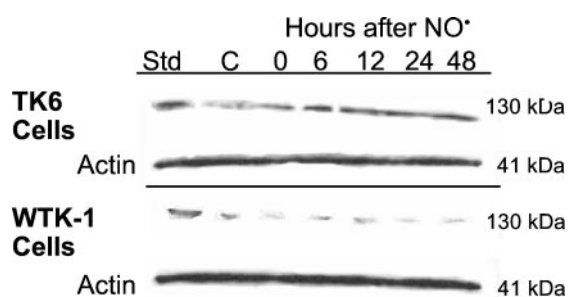


Fig. 7. Apaf-1 protein levels in TK6 and WTK-1 cells treated with NO• at 533 nM/s for 2 h, detected by Western blots. Lysates (50 μ g) of Jurkat cells treated with 4 μ M staurosporine served as a positive control.

Substantial amounts were detectable 6 h after treatment and levels increased through 48 h, except for a transient decline at 24 h (Fig. 6). Apaf-1 protein was detectable in argon-treated control cells of both types; after NO• treatment, levels increased progressively through 48 h in TK6 cells, but remained essentially unchanged in WTK-1 cells during the same time (Fig. 7). The relatively high levels of XIAP protein in WTK-1 cells did not change significantly during the 24-h period after treatment, whereas they declined markedly in TK6 cells (Fig. 8).

Discussion

We found that DNA double-strand breaks, fragmentation, and apoptosis detectable 8–48 h after NO• treatment were more extensive in TK6 cells expressing wild-type p53 than in WTK-1 cells expressing mutant p53. In contrast, both spontaneous and induced mutant fractions at the *HPRT* and *TK1* genes were much lower in TK6 cells. NO• treatment induced mitochondrial depolarization and cytochrome *c* release in both cell lines. In addition, increased levels of the Apaf-1 protein and decreased levels of the XIAP protein were observed in TK6 cells but not in WTK-1 cells after exposure. These results show that p53 status is an important modulator of NO•-induced mutagenesis and apoptosis and suggest that Apaf-1 and XIAP are regulated by p53 and may play important roles in p53-mediated apoptosis in these human lymphoblastoid cell types. In this investigation, NO• gas was delivered for 2 h through a well controlled membrane delivery system into stirred cell suspensions at dose rates of 100–533 nM/s, similar to estimated levels existing *in vivo* under pathological conditions (20, 31). This delivery method was used to circumvent confounding issues that might be introduced by NO• exposure by way of donor drugs or bolus administration.

Dysfunction of p53 has been associated with delayed apoptosis and increased genomic instability induced by ionizing irradiation and DNA-damaging agents (11–16). Previous investigators have

shown that wild-type p53 protein in TK6 cells was increased by ionizing radiation or other DNA-damaging agents, whereas the high basal level of mutant p53 protein in WTK-1 cells showed no further increase after the same treatments (15, 32). We found that the mutagenic response to NO• treatment at both the *HPRT* and *TK1* loci was much more pronounced in WTK-1 cells than in TK6 cells, confirming that p53 function significantly modulates mutagenesis in these human lymphoblasts. Although mechanisms responsible for the difference in response are unknown, they may include impairment of p53-dependent apoptosis triggered by DNA damage, because our results show that NO• induced a delayed and diminished apoptotic response in p53 mutant compared with wild-type cells (Fig. 5A). Inappropriate survival of cells containing damaged DNA could result in accumulation of mutations including large-scale genetic rearrangements (13, 33). Alternatively, the mutational response could be altered by direct participation of p53 in repair of DNA damage through regulation of recombination-mediated mutagenic pathways (34). The importance of this factor is suggested by the difference in processing of DNA damage, reflected in DNA strand breaks and fragmentation, induced by NO• in the two cell lines. In addition, the mutant p53 of WTK-1 cells may also exhibit so-called “gain of function” properties in apoptosis and/or mutagenesis (35).

The presence of more extensive DNA double-strand breaks and fragmentation by NO• in TK6 cells than in WTK-1 cells was in general agreement with our recent findings in the same cell lines treated with peroxynitrite generated from SIN-1 (36). In addition, previous investigators have found that TK6 cells were more sensitive to formation of NO•-induced DNA single-strand breaks than Chinese hamster ovary cells (CHO-AA8) in which the *p53* gene was either inactive or mutated (21), and that DNA fragmentation induced by ionizing radiation was more extensive in TK6 cells than in WTK-1 cells (15). Our results also revealed that spontaneous as well as NO• and 4-NQO-induced mutagenesis were significantly higher in the *TK1* gene than in the *HPRT* gene of WTK-1 cells ($P < 0.05$ – 0.01). Differential effects of mutant p53 on mutability of these loci have been attributed to the hemizyosity of *HPRT* versus the heterozygosity of *TK1* (14). Because these cells carry only one copy of *HPRT*, the efficiency of recombination-mediated mutagenesis at this locus is limited. In addition, deletions around *HPRT* tend to be lethal, which also limits the accumulation of viable mutants containing large-scale changes (34). Analysis of the physical structures of x-ray-induced *TK1* mutants (34) revealed that greater mutability at this locus was associated with a higher frequency of inter- and intramolecular recombination events, suggesting that a recombinational repair system was functioning at a higher level in WTK-1 cells than in TK6 cells, and that the increase in *TK1* mutagenesis could be attributed, in part, to mitotic recombination. Our findings in NO•-treated cells are also consistent with these interpretations. The recent observation (37) that NO• was comparable to UV in its ability to induce recombination in *Escherichia coli* is also of interest in this context.

Estimated physiological levels of NO• production (11 nM/s) have been shown to inhibit mitochondrial permeability transition pore opening reversibly, whereas superphysiological release rates ($>2 \mu$ M/s) accelerate opening (31). Our data revealed that high nanomolar concentrations per second of NO• induced mitochondrial membrane depolarization and cytochrome *c* release in wild-type (TK6) and mutant p53 (WTK-1) human lymphoblasts. Activated p53 regulates the expression of genes that control mitochondrial membrane permeability and, therefore, release of cytochrome *c* during apoptosis (38). In our experiments, a substantial amount of cytosolic cytochrome *c* was detected in both cell lines at 6 h (Fig. 6), whereas the MMP loss was minimal at 8 h (Fig. 5). Amounts of cytosolic cytochrome *c* were essentially equal, despite the higher MMP loss in WTK-1

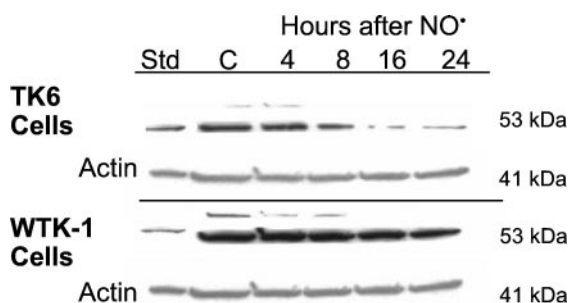


Fig. 8. XIAP protein levels in TK6 and WTK-1 cells treated with NO• at 533 nM/s for 2 h, detected by Western blots. Lysates (25 μ g) of Jurkat cells treated with 4 μ M staurosporine served as a positive control.

versus TK6 cells. These findings are consistent with previous reports that cytochrome *c* release was independent of MMP loss after treatment of cells with diverse agents (39, 40). In addition, many investigations have revealed that the antiapoptotic proteins Bcl-2 and Bcl-x/l block p53-regulated release of cytochrome *c* from mitochondria (6, 10, 38). If Bcl-2 and Bcl-x/l were reduced by NO[•] treatment in TK6 cells, this effect could also contribute to the higher cytochrome *c* release observed.

Elevated expression of the Apaf-1 protein was observed only in TK6 cells after NO[•] treatment. Apaf-1 plays a central role in the common events of mitochondria-dependent apoptosis in most death pathways (41). Two recent reports indicate that Apaf-1 is a direct transcriptional target of p53 and an essential downstream effector of p53-mediated apoptosis (32, 42). Our results complement and extend this finding at the protein level, suggesting that p53 may sensitize cells to apoptosis by increasing expression of the Apaf-1 protein. Exposure of isolated rat liver mitochondria to an NO[•] donor leads to mitochondrial depolarization and cytochrome *c* release (31). Our data also suggest that

NO[•] may damage mitochondria directly or indirectly in both TK6 and WTK-1 cells, leading to cytochrome *c* release that may be not mediated by p53.

XIAP is the most potent caspase inhibitor in the IAP family and inhibits both the initiator caspase 9 and the effector caspases 3 and 7 (8). Its caspase-inhibiting activity is negatively regulated by at least two XIAP-interacting proteins, XAF1 (XIAP-associated factor 1) and mitochondrial proapoptotic factor Smac/DIABLO (8, 43). We found that NO[•] treatment reduced levels of the XIAP protein in TK6 cells, but did not alter its level in WTK-1 cells, suggesting that XIAP may be negatively regulated by p53 in human lymphoblasts. The potential relevance of this observation is underscored by the finding that down-regulation of XIAP protein induces apoptosis in chemoresistant human ovarian cancer cells (44). We are currently further investigating NO[•]-induced apoptotic signaling pathways, with particular emphasis on the involvement of IAP gene products.

This work was supported by National Cancer Institute Grant 5 P01 CA26731.

- Brune, B., von Knethen, A. & Sandau, K. B. (1998) *Eur. J. Pharmacol.* **351**, 261–272.
- Kim, P. K., Zamora, R., Petrosko, P. & Billiar, T. R. (2001) *Int. Immunopharmacol.* **1**, 1421–1441.
- Messmer, U. K. & Brune, B. (1995) *Biochem. J.* **319**, 299–305.
- Hortelano, S., Dallaporta, B., Zamzami, N., Hirsch, T., Susin, S. A., Marzo, I., Bosca, L. & Kroemer, G. (1997) *FEBS Lett.* **410**, 373–377.
- Vousden, K. H. (2000) *Cell* **103**, 691–694.
- Shi, Y. (2001) *Nat. Struct. Biol.* **8**, 394–401.
- Ashkenazi, A. & Dixit, V. M. (1998) *Science* **281**, 1305–1308.
- Deveraux, Q. L. & Reed, J. C. (1999) *Genes Dev.* **13**, 239–252.
- Levine, A. J. (1997) *Cell* **88**, 323–331.
- Stewart, Z. A. & Pietenpol, J. A. (2001) *Chem. Res. Toxicol.* **14**, 243–263.
- Xia, F., Wang, X., Wang, Y. H., Tsang, N. M., Yandell, D. W., Kelsey, K. T. & Liber, H. L. (1995) *Cancer Res.* **55**, 12–15.
- Zhen, W., Denault, C. M., Loviscek, K., Walter, S., Geng, L. & Vaughan, A. T. (1995) *Mutat. Res.* **346**, 85–92.
- Greenwood, S. K., Armstrong, M. J., Hill, R. B., Bradt, C. I., Johnson, T. E., Hilliard, C. A. & Galloway, S. M. (1998) *Mutat. Res.* **401**, 39–53.
- Xia, F. & Liber, H. L. (1997) *Mutat. Res.* **373**, 87–97.
- Yu, Y. & Little, J. B. (1998) *Cancer Res.* **58**, 4277–4281.
- Amundson, S. A., Xia, F., Wolfson, K. & Liber, H. L. (1993) *Mutat. Res.* **286**, 233–241.
- Hickman, M. J. & Samson, L. D. (1999) *Proc. Natl. Acad. Sci. USA* **96**, 10764–10769.
- Soengas, M. S., Alarcon, R. M., Yoshida, H., Giaccia, A. J., Hakem, R., Mak, T. W. & Lowe, S. W. (1999) *Science* **284**, 156–159.
- Jia, L., Srinivasula, S. M., Liu, F. T., Newland, A. C., Fernandes-Alnemri, T., Alnemri, E. S. & Kelsey, S. M. (2001) *Blood* **98**, 414–421.
- Patel, R. P., McAndrew, J., Sellak, H., White, C. R., Jo, H., Freeman, B. A. & Darley-Usmar, V. M. (1999) *Biochim. Biophys. Acta* **1411**, 385–400.
- Burney, S., Tamir, S., Gal, A. & Tannenbaum, S. R. (1997) *Nitric Oxide* **1**, 130–144.
- Hickman, C. W. & Tabor, H. (1985) *Microbiol. Rev.* **49**, 81–99.
- Tamir, S., Lewis, R. S., de Rojas Walker, T., Deen, W. M., Wishnok, J. S. & Tannenbaum, S. R. (1993) *Chem. Res. Toxicol.* **6**, 895–899.
- Green, L. C., Wagner, D. A., Glogowski, J., Skipper, P. L., Wishnok, J. S. & Tannenbaum, S. R. (1982) *Anal. Biochem.* **126**, 131–138.
- Liber, H. L. & Thilly, W. G. (1982) *Mutat. Res.* **94**, 467–485.
- Olive, P. L., Banath, J. P. & Durand, R. E. (1990) *Radiat. Res.* **122**, 86–94.
- Salvioli, S., Ardizzone, A., Franceschi, C. & Cossarizza, A. (1997) *FEBS Lett.* **411**, 77–82.
- Ankarcrona, M., Dypbukt, J. M., Bonfoco, E., Zhivotovsky, B., Orrenius, S., Lipton, S. A. & Nicotera, P. (1995) *Neuron* **15**, 961–973.
- Bortner, C. D. & Cidlowski, J. A. (1999) *J. Biol. Chem.* **274**, 21953–21962.
- Bossy-Wetzel, E. & Green, D. R. (2000) *Methods Enzymol.* **322**, 235–242.
- Brookes, P. S., Salinas, E. P., Darley-Usmar, K., Eiserich, J. P., Freeman, B. A., Darley-Usmar, V. M. & Anderson, P. G. (2000) *J. Biol. Chem.* **275**, 20474–20479.
- Robles, A. I., Bemmels, N. A., Foraker, A. B. & Harris, C. C. (2001) *Cancer Res.* **61**, 6660–6664.
- Schwartz, J. L., Jordan, R., Sedita, B. A., Swenningson, M. J., Banath, J. P. & Olive, P. L. (1995) *Mutagenesis* **10**, 227–233.
- Xia, F., Amundson, S. A., Nickoloff, J. A. & Liber, H. L. (1994) *Mol. Cell Biol.* **14**, 5850–5857.
- Sigal, A. & Rotter, V. (2000) *Cancer Res.* **60**, 6788–6793.
- Li, C. Q., Trudel, L. J. & Wogan, G. N. (2002) *Chem. Res. Toxicol.* **15**, 527–535.
- Spek, E., Wright, T. L., Stitt, M. S., Taghizadeh, N. R., Tannenbaum, S. R., Marinus, M. G. & Engelward, B. P. (2001) *J. Bacteriol.* **183**, 131–138.
- Moll, U. M. & Zaika, A. (2001) *FEBS Lett.* **493**, 65–69.
- Kluck, R. M., Bossy-Wetzel, E., Green, D. R. & Newmeyer, D. D. (1997) *Science* **275**, 1132–1136.
- Chiu, S. M. & Oleinick, N. L. (2001) *Br. J. Cancer* **84**, 1099–1106.
- Yoshida, H., Kong, Y. Y., Yoshida, R., Elia, A. J., Hakem, A., Hakem, R., Penninger, J. M. & Mak, T. W. (1998) *Cell* **94**, 739–750.
- Moroni, M. C., Hickman, E. S., Denchi, E. L., Caprara, G., Colli, E., Cecconi, F., Muller, H. & Helin, K. (2001) *Nat. Cell Biol.* **3**, 552–558.
- Holcik, M., Gibson, H. & Korneluk, R. G. (2001) *Apoptosis* **6**, 253–261.
- Sasaki, H., Sheng, Y., Kotsuji, F. & Tsang, B. K. (2000) *Cancer Res.* **60**, 5659–5666.